

# Testing the tensor-vector-scalar Theory with the latest cosmological observations

Xiao-dong Xu, Bin Wang, Pengjie Zhang

*IFSA Collaborative Innovation Center,  
Department of Physics and Astronomy,  
Shanghai Jiao Tong University, Shanghai 200240, China*

## Abstract

The tensor-vector-scalar (TeVeS) model is considered a viable theory of gravity. It produces the Milgrom's modified Newtonian dynamics in the nonrelativistic weak field limit and is free from ghosts. This model has been tested against various cosmological observations. Here we investigate whether new observations such as the galaxy velocity power spectrum measured by 6dF and the kinetic Sunyaev Zel'dovich effect power spectrum measured by ACT/SPT can put further constraints on the TeVeS model. Furthermore, we perform the test of TeVeS cosmology with a sterile neutrino by confronting to *Planck* data, and find that it is ruled out by cosmic microwave background measurements from the *Planck* mission.

PACS numbers: 98.80.-k, 04.50.Kd

## I. INTRODUCTION

The convincing observational evidences from the scale of galaxies to the scale of the cosmic microwave background (CMB) radiation accumulated over the past few decades raised the missing mass problem: there is a mismatch between the dynamics and distribution of visible matter [1–10]. To explain this problem, one usually postulates the existence of a new form of matter in nature, called dark matter (DM). DM is considered nonbaryonic and does not emit light or interact with electromagnetic field. For now people only detect DM through its gravitational effect. Traditionally, DM can be classified as “hot dark matter,” which is composed of relativistic particles such as massive neutrinos; “cold dark matter” (CDM), which is composed of very massive slowly moving and weakly interacting particles; and in between the possible “warm dark matter,” which is also sometimes considered. One attributes the observed extra gravitational force to the DM component whose abundance greatly exceeds the visible matter. In the standard  $\Lambda$ CDM model, DM contributes about 25% to the total energy budget in the Universe. The discrepancy between the dynamics and distribution of visible matter happens on galactic to cosmological scales. Decades after the proposal of DM, it was discovered that the expansion of our Universe is accelerating, which calls for another new substance, dark energy (DE), to contribute the mysterious missing energy at cosmological scales.

Einstein’s general relativity (GR) has been vigorously tested in the Solar System, but on galaxy or larger scales its validity has not been completely proved. Considering that the law of gravity plays a fundamental role at every instance where discrepancies have been observed, it is possible that the phenomena attributed to DM and DE are just a different theory of gravity in disguise. The research relating to modifications of gravity theory is not extensive. In the literature, modified gravity theories usually contain a Newtonian limit for the low velocity, weak potential case. Considering that the mass discrepancy problem appears on extragalactic scales where Newtonian gravity is expected to be a good approximation, these theories cannot solve the problem without the help of the invisible matter component. This has been resolved in the Milgrom’s modified Newtonian dynamics(MOND) proposal[11–13], which assumes that Newtonian gravity fails in low acceleration cases. Instead, the acceleration  $a$  induced by the gravitational force was proposed as  $\tilde{\mu}(a/a_0)a = -\nabla\Phi_N$ , where  $a_0$  is a characteristic acceleration scale, and  $\Phi_N$  is the usual Newtonian potential.  $\tilde{\mu}(x) \simeq x$  for  $x \ll 1$  and  $\tilde{\mu}(x) \rightarrow 1$  for  $x \gg 1$ . In laboratory and solar system experiments,  $a \gg a_0$ , MOND returns to the Newtonian dynamics; while in the extragalactic regime where  $a \ll a_0$ , the acceleration squared is proportional to the gravitational force. MOND is extremely successful in explaining galactic rotation curve[14–20] and the Tully-Fisher law [21, 22]. Some other predictions of MOND can be found in[23–28].

To be able to make predictions for cosmological observations, a relativistic theory of MOND is required. After some early attempts[29–33], Bekenstein succeeded in constructing tensor-vector-scalar (TeVeS) theory[34], which is a relativistic theory of gravity and produces MOND in the nonrelativistic weak field limit. The name comes from the fact that the theory contains a scalar and a vector field in addition to the metric (a tensor field). TeVeS theory has proven successful in explaining the astrophysical data at scales larger than that of the Solar System without the need of an excessive amount of invisible matter [35–43]. Moreover, TeVeS theory has proven to be free of ghosts[44], which makes TeVeS, including its nonrelativistic limit, a viable theory of gravity.

In order to predict large scale structure observations in TeVeS theory, we need the linear

cosmological perturbation theory in TeVeS, which was constructed in a pioneer work[45]. Based on the perturbation theory, the large scale structure in TeVeS cosmology was first discussed in [46], where it was argued that perturbations of the scalar field may induce enhanced growth in the matter perturbations. Analytic explanation of the growth of structure was subsequently given in [47], where it was claimed that the perturbations of the vector field are key to the enhanced growth. It was further clarified in [26] that even if the contribution of the TeVeS fields to the background Friedmann equations is negligible, one can still get a growing mode that drives structure formation. This explains analytically the numerical results in [46].

It is of great interest to examine whether TeVeS theory can give predictions for large scale structure similar to the  $\Lambda$ CDM model and whether it is compatible with cosmological observations. In [48], Reyes *et al.* reported the measurement of  $E_G$ , an estimator of the ratio of the Laplacian of gravitational potential to the peculiar velocity divergence[49], using a sample of 70,205 luminous red galaxies in the redshift range [0.16, 0.47] from the Sloan Digital Sky Survey. They claimed that the original Bekenstein's TeVeS model is excluded at  $2.5\sigma$ . Since  $E_G$  measures the ratio of two types of perturbations, it is insensitive to the overall amplitude of perturbation. Other than  $E_G$ , observations such as the galaxy velocity power spectrum and the kinetic Sunyaev Zel'dovich (kSZ) effect are sensitive to the perturbation amplitude. It is intriguing to investigate whether these probes can put complementary constraints on TeVeS and modified gravity theories in general. This motivates us to further test TeVeS against these complementary observations in large scale structure and examine whether these tests can distinguish TeVeS from  $\Lambda$ CDM, which serves as the first motivation of the paper.

The mechanism of structure growth in TeVeS theory is different from that in the  $\Lambda$ CDM model. In  $\Lambda$ CDM, after decoupling from photons, baryons fall into the gravitational wells induced by CDM. While in TeVeS, the growth of perturbations is driven by the vector field whose perturbation grows rapidly after recombination[47]. This may lead to difference in the growth of baryon density perturbation and the amplitude of the matter peculiar velocity. The change on the matter peculiar velocity can further induce temperature fluctuations on the CMB map at small scales via the conventional kSZ effect. The kSZ effect is generated through CMB photons scattering off free electrons in the diffuse intergalactic medium and the unresolved cluster population. The study of the kSZ effect is appealing, since it can be observed with the new generation CMB experiments. Recently, the kSZ effect has been found as a potential probe of reionization, the radial inhomogeneities in the Lemaitre-Tolman-Bondi cosmology[50], the missing baryon problem[51], the dark flow[52] and the interaction between the dark sectors[53]. Here, we further investigate the kSZ effect in the frame of TeVeS theory, and disclose whether it can be used to constrain the TeVeS model.

In addition to the signatures in the kSZ effect, we also consider the growth rate of baryon density perturbation in TeVeS theory. The growth rate is generally a function of the cosmic scale factor  $a$  and the comoving wave number  $k$ , defined as  $f(k; a) = d \ln \delta(k; a) / d \ln a$ . Although the temporal dependence of the growth rate has been readily measured by galaxy surveys using redshift-space distortion measurements[54–56], its spatial dependence is currently only weakly constrained[57–59]. However the theoretical study of the latter has undoubted importance, for it is a critical test of theories of gravity. A characteristic prediction of  $\Lambda$ CDM is a scale-independent growth rate, while modified gravity models commonly induce a scale dependence in the growth rate. Thus the measurement of the growth rate, especially its spatial dependence can distinguish modified gravity theories from the stan-

standard  $\Lambda$ CDM model, even if they produce the same expansion history of the Universe. In this work we examine the scale dependence of growth rate in TeVeS and see whether TeVeS can be distinguished from the  $\Lambda$ CDM model using current observations. Since changes in the density/velocity growth rate and scale dependence of the growth rate are generically expected in modified gravity models, the tests we carry out for the TeVeS model can, in principle, be applied to other modified gravity models. Our study on the TeVeS model here then serves as an example to demonstrate possible impacts of these new observations on tests of general relativity at cosmological scales.

The observational data of the probes we proposed above suffer large uncertainties in present observations. Thus, in order to put a tight constraint on the TeVeS model with current data, it is necessary to confront the model with other complementary observations on different scales and redshifts whose precise measurements are already available. For this purpose we extend our study of the TeVeS cosmology to the CMB since the most accurate observational data on cosmological scales to date come from the CMB experiments. In [46] the CMB angular power spectrum for the TeVeS was first calculated numerically by solving the linear Boltzmann equations in the case of TeVeS theory. By using the initial conditions close to adiabatic, it was found that the power spectrum provides poor fit to observations compared to the  $\Lambda$ CDM model. It was observed that if a cosmological constant and/or three massive neutrinos are incorporated into the matter budget, the first peak of the CMB angular power spectrum could be located at the right position[46]. Later it was argued that by including a fourth sterile neutrino, a MOND-like theory can have good fits to the CMB angular power spectrum[60]. However, in this research, it was assumed that there were no MOND effects before recombination, so that the MOND effects do not influence the CMB power spectrum. Thus, it would be fair to say that their fitting result has nothing to do with TeVeS features. In this work, we take into account the full TeVeS features and their corresponding influences on the CMB. We examine whether we can get a good fit to current CMB observations by including the cosmological constant and the fourth neutrino. Considering the high precision of *Planck* results, we expect that the CMB observations can give tight constraints on TeVeS cosmology.

The paper is organized as follows. In Sec.II, we go over the TeVeS model and its application in cosmology. In the following section, we examine the evolution of the density perturbation (Sec.III A) and the baryon peculiar velocity (Sec.III B) in TeVeS theory. In Sec.III C we show that the kSZ effect is a potential probe to constrain the TeVeS model. In Sec.III D, we focus on the scale dependence of the growth rate in the TeVeS model and compare with that of the  $\Lambda$ CDM model and observational data. In Sec.IV, we concentrate on its influence on the CMB angular power spectrum in the presence of the sterile neutrino and we confront the TeVeS model with *Planck* data. Finally we draw the conclusions in Sec.V.

## II. FUNDAMENTALS OF TEVES THEORY

There are two metrics in Bekenstein's TeVeS theory[34]. In addition to the Einstein frame metric  $\tilde{g}_{\mu\nu}$  whose dynamics is governed by the standard Einstein-Hilbert action, it also has the matter frame metric  $g_{\mu\nu}$ . These two metrics are related through[34]

$$g_{\mu\nu} = e^{-2\phi}\tilde{g}_{\mu\nu} - 2\sinh(2\phi)A_\mu A_\nu, \quad (1)$$

where  $\phi$  is a scalar field and  $A_\mu$  is a vector field. The vector field is required to be unit timelike in the Einstein frame,  $\tilde{g}^{\mu\nu} A_\mu A_\nu = -1$ . The dynamics of the scalar and vector fields is given by the action  $S_\phi$  and  $S_A$ :

$$S_\phi = -\frac{1}{16\pi G} \int d^4x \sqrt{-\tilde{g}} [\mu(\tilde{g}^{\mu\nu} - A^\mu A^\nu) \tilde{\nabla}_\mu \phi \tilde{\nabla}_\nu \phi + V(\mu)], \quad (2)$$

$$S_A = -\frac{1}{32\pi G} \int d^4x \sqrt{-\tilde{g}} [K_B F_{\mu\nu} F^{\mu\nu} - 2\lambda(A_\mu A^\mu + 1)], \quad (3)$$

where  $\mu$  is a nondynamical dimensionless scalar field,  $F_{\mu\nu} \equiv 2\tilde{\nabla}_{[\mu} A_{\nu]}$ ,  $F^{\mu\nu} = \tilde{g}^{\mu\alpha} \tilde{g}^{\nu\beta} F_{\alpha\beta}$ ,  $A^\mu = \tilde{g}^{\mu\nu} A_\nu$ ,  $\lambda$  is a Lagrange multiplier ensuring the unit timelike constraint on  $A_\mu$  and  $K_B$  is a dimensionless constant.  $G$  is the bare gravitational constant, whose value does not equal to the measured Newton's constant. The relation between the gravitational constant and Newton's constant depends on the quasistatic, spherically symmetric solution to the TeVeS field equations and the free function  $V(\mu)$  [34, 61–63].  $V(\mu)$  typically depends on a scale  $l_B$ . In Bekenstein's original work, he proposed [34]

$$\frac{dV}{d\mu} = -\frac{3}{32\pi l_B^2 \mu_0^2} \frac{\mu^2(\mu - 2\mu_0)^2}{\mu_0 - \mu}, \quad (4)$$

where  $\mu_0$  is a dimensionless constant. A generalization to this function was proposed in [62]. Sanders [64] and Angus *et al.* [65] suggested alternative functions that also lead to MOND.

The action for matter fields is usually written in the matter frame, where it takes the same form as in GR. Hence the matter frame metric is sometimes called the physical metric. Generically denoting the matter fields by  $\chi^A$ , we have

$$S_m = \int d^4x \sqrt{-g} \mathcal{L}[g, \chi^A, \partial\chi^A]. \quad (5)$$

### A. Background dynamics in TeVeS cosmology

The solutions for the homogeneous and isotropic universe in TeVeS theory have been studied in [34, 62, 66–69]. Assuming that the spacetime is flat, the physical metric takes the form

$$ds^2 = a^2(-d\eta^2 + dr^2), \quad (6)$$

and the Einstein metric has the similar form

$$d\tilde{s}^2 = b^2(-e^{-4\phi} d\tilde{\eta}^2 + d\tilde{r}^2). \quad (7)$$

$a$  and  $b$  are the scale factors in the matter and Einstein frames. They are related through  $a = b e^{-\phi}$ . In the Einstein frame, the Friedmann equation reads [45]:

$$3\frac{\dot{b}^2}{b^2} = a^2 \left[ \frac{1}{2} e^{-2\phi} (\mu V' + V) + 8\pi G e^{-4\phi} \rho \right], \quad (8)$$

where  $\rho$  is the matter energy density that does not include the scalar field. The vector field is not dynamical in FLRW cosmology. It always points to the time direction, and does not

contribute to the total energy density. The background dynamics is completely described if we have the equation of motion for  $\phi$ ,

$$\ddot{\phi} = \dot{\phi} \left( \frac{\dot{a}}{a} - \dot{\phi} \right) - \frac{1}{U} \left[ 3\mu \frac{\dot{b}}{b} \dot{\phi} + 4\pi G a^2 e^{-4\phi} (\rho + 3P) \right], \quad (9)$$

where  $U \equiv \mu + 2V'/V''$  and  $P$  denotes the pressure that does not include the pressure of the scalar field.

In the matter frame, the Hubble parameter is defined as  $H \equiv \frac{\dot{a}}{a^2}$ , where the dot denotes the derivative with respect to the conformal time in the matter frame. The effective Friedmann equation then reads[45]

$$3H^2 = 8\pi G_{\text{eff}}(\rho + \rho_\phi), \quad (10)$$

where the effective gravitational constant is  $G_{\text{eff}} = G \frac{e^{-4\phi}}{(1 + \frac{d\phi}{d \ln a})^2}$ . The effective energy density of the scalar field is

$$\rho_\phi = \frac{1}{16\pi G} e^{2\phi} (\mu V' + V). \quad (11)$$

If the free function  $V$  takes the form of (4), the scalar field energy density will track the matter energy density[26, 46, 47]. Defining the effective density fraction as  $\Omega_\phi = \frac{\rho_\phi}{\rho + \rho_\phi}$ , the tracker is  $\Omega_\phi = \frac{(1+3w)^2}{6(1-w)^2 \mu_0}$ , where  $w$  is the equation of state of the background matter field. The typical value of  $\mu_0$  has the order of  $10^2$ , so the scalar field is always subdominant in the history of our Universe.

We are free to add an arbitrary integration constant to  $V$ . This will only change the Lagrangian of the scalar field by a constant, thus has no influence on the field equations and the evolution of the gravitational fields. Adding a constant in  $V$  is equivalent to include a cosmological constant in the effective Friedmann equation (10). This leads to the desired accelerated expansion of our Universe.

## B. Linear perturbation theory in TeVeS cosmology

In this subsection we go over the linear perturbation theory on the background described above. This will allow us to link TeVeS theory with observations of structure formation on large scale as well as the CMB anisotropies.

The linear perturbation theory for TeVeS cosmology was first constructed in [45]. We employ the formalism in [45] and consider only scalar perturbations.

We work under the conformal synchronous gauge, for which  $\delta g_{00} = \delta g_{0i} = 0$  and  $\delta g_{ij} = 2H_L \delta_{ij} + (\partial_i \partial_j - \frac{1}{3} \delta_{ij} \Delta) H_T$ . It is conventional to write in Fourier space  $H_L = h/6$  and  $H_T = -(h + 6\eta)/k^2$ . The evolution equations for the matter density contrast and velocity take the same forms as GR in the matter frame

$$\dot{\delta} = -3 \frac{\dot{a}}{a} (C_s^2 - w) \delta - (1 + w) \left( k^2 \theta + \frac{1}{2} \dot{h} \right), \quad (12)$$

$$\dot{\theta} = -\frac{\dot{a}}{a} (1 - 3w) \theta + \frac{C_s^2}{1 + w} \delta - \frac{\dot{w}}{1 + w} \theta - \frac{2}{3} k^2 \Sigma. \quad (13)$$

We denote the perturbation to the scalar field by  $\varphi$ , so that  $\phi = \bar{\phi} + \varphi$ . The vector field perturbation is defined as  $A_\mu \equiv \bar{A}_\mu + ae^{-\bar{\phi}}\alpha_\mu$ . Its scalar mode is  $\Delta\alpha = \nabla \cdot \vec{\alpha}$ . The evolution equations for the scalar field are given by

$$\dot{\varphi} = -\frac{1}{2U}ae^{-\bar{\phi}}\gamma - \dot{\bar{\phi}}\varphi, \quad (14)$$

$$\begin{aligned} \dot{\gamma} = & -3\frac{\dot{b}}{b}\gamma + \frac{\bar{\mu}}{a}e^{-3\bar{\phi}}k^2(\varphi + \dot{\bar{\phi}}\alpha) + \frac{e^{\bar{\phi}}}{a}\bar{\mu}\dot{\bar{\phi}}[\dot{h} + 6\dot{\varphi} + 2k^2(1 - e^{4\bar{\phi}})\alpha] \\ & + 8\pi Gae^{-3\bar{\phi}}[\delta\rho + 3\delta P - 3(\bar{\rho} + 3\bar{P})\varphi]. \end{aligned} \quad (15)$$

The equations for the perturbed vector field obey

$$\dot{\alpha} = E - \varphi + \left(\dot{\bar{\phi}} - \frac{\dot{a}}{a}\right)\alpha, \quad (16)$$

$$K_B\left(\dot{E} + \frac{\dot{b}}{b}E\right) = -\bar{\mu}\dot{\bar{\phi}}(\varphi - \dot{\bar{\phi}}\alpha) + 8\pi Ga^2(1 - e^{-4\bar{\phi}})(\bar{\rho} + \bar{P})(\theta - \alpha). \quad (17)$$

The perturbed modified Einstein equations yield

$$2k^2(\varphi - \eta) + e^{4\bar{\phi}}\frac{\dot{b}}{b}\left(\dot{h} + 2k^2(1 - e^{-4\bar{\phi}})\alpha + 6\frac{\dot{a}}{a}\varphi\right) + ae^{3\bar{\phi}}\left(\dot{\bar{\phi}} - \frac{3}{U}\frac{\dot{b}}{b}\right)\gamma \quad (18)$$

$$-K_Bk^2E = 8\pi Ga^2\bar{\rho}(\delta - 2\varphi),$$

$$2k^2\dot{\eta} - 2k^2\left(\frac{\dot{a}}{a} + \bar{\mu}\dot{\bar{\phi}}\right)\varphi + \frac{k^2}{U}ae^{-\bar{\phi}}\gamma = 8\pi Ga^2e^{-4\bar{\phi}}(\bar{\rho} + \bar{P})k^2\theta. \quad (19)$$

To solve these perturbation equations, we need to specify the initial conditions. In [70] the adiabatic initial conditions of scalar mode perturbations during the radiation era were proposed. In our numerical computations in the following discussions we adopt those initial conditions for the selected special potential (4).

### III. LARGE SCALE STRUCTURE IN TEVES THEORY

#### A. The growth of the baryon density fluctuation

The growth of structure in TeVeS theory was first discussed in [46]. It was reported that with the decrease of the TeVeS parameters  $K_B$ ,  $l_B$  and  $\mu_0$ , the small scale power spectrum of the baryon density fluctuations can be boosted to mimic that in the adiabatic  $\Lambda$ CDM model. In [47] it was pointed out that the growth of structure in the TeVeS is mainly due to the vector field. In [26], it was further clarified that even if the contribution of the TeVeS fields to total energy budget in the background FLRW universe is negligible, we can still have a growing mode of density fluctuations that drives structure formation.

Although the matter power spectrum in TeVeS theory can mimic that in  $\Lambda$ CDM cosmology, the mechanism of structure growth in two models is different. In the  $\Lambda$ CDM model, after decoupling from photons, baryons fall into the gravitational wells induced by CDM. In TeVeS theory, the growth of perturbations is mainly driven by the vector field that grows rapidly after recombination. Thus it may be possible to distinguish them by studying the evolution history of the perturbations.

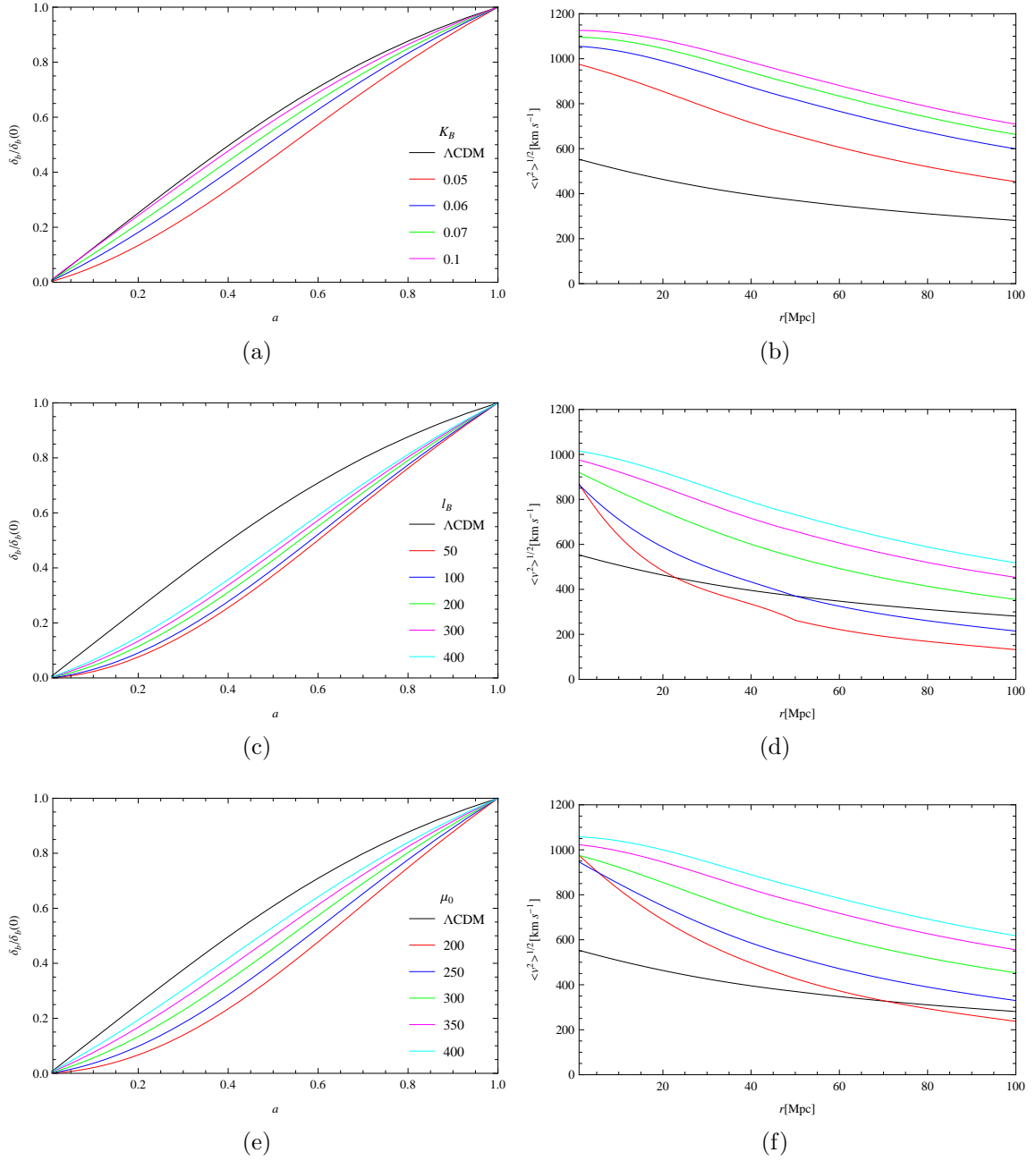


FIG. 1: The figures on the left column are the evolutions of  $\delta_b$  for  $k = 0.1\text{Mpc}^{-1}$ , normalized to its present value; on the right column is the root mean square(rms) dispersion of baryon peculiar velocities. The black curves correspond to the fiducial  $\Lambda\text{CDM}$  model. The colored curves are for TeVeS models with different parameters. The curves in the figures on the same row follow the same convention. The TeVeS parameters are  $K_B = 0.05$ ,  $l_B = 300$  and  $\mu_0 = 300$  if not specified. The fourth neutrino abundance is  $\Omega_\nu h^2 = 0.15$

In the left column of Fig.1, we demonstrate the evolutions of baryon density perturbation in synchronous gauge,  $\delta_b$ , in TeVeS models. The density perturbations are evaluated for  $k = 0.1\text{Mpc}^{-1}$ . For comparison, we also plot the evolution of  $\delta_b$  in the fiducial  $\Lambda\text{CDM}$



model. We take the cosmological parameters  $\Omega_b h^2 = 0.022$ ,  $\Omega_c h^2 = 0.12$ ,  $h = 0.68$ ,  $\tau = 0.09$ ;  $n_s = 0.96$  and  $\ln(10^{10} A_s) = 3.1$ , where the Hubble constant  $H_0 = 100 h \text{ km} \cdot \text{s}^{-1} \cdot \text{Mpc}^{-1}$ ,  $\tau$  is the optical depth to the last scattering surface,  $n_s$  and  $A_s$  are the spectral index and amplitude of the primordial power spectrum. We use these parameters for the fiducial  $\Lambda$ CDM model and TeVeS models (except  $\Omega_c h^2 = 0$ ) throughout this paper. We also introduce one sterile neutrino in addition to three massless neutrinos in the TeVeS cosmology, as [60] suggested in order to fit the CMB observations. In the calculations  $\Omega_\nu = 0.15$ . As we expected, the growth rate of  $\delta_b$  in TeVeS theory differs from that in the  $\Lambda$ CDM model. In most cases, the perturbations grow faster in TeVeS theory than in the  $\Lambda$ CDM model at low redshifts. And the smaller the TeVeS parameters are, the more the growth rate deviates from the  $\Lambda$ CDM model. The growth rate is especially sensitive to  $K_B$  when it is small. Thus observing the structure growth can also help in constraining the TeVeS parameters.

Besides the evolution of the growth rate, its spatial dependence is also attractive in distinguishing TeVeS cosmology from  $\Lambda$ CDM. We discuss this topic in the last subsection below.

## B. The peculiar velocity

The peculiar velocity is related to the time derivative of the density perturbation in the linear perturbation theory. In Newtonian gauge, we have the relation

$$v_b^{(N)} = -\frac{\dot{\delta}_b^{(N)}}{k} = -aHf^{(N)}\frac{\delta_b^{(N)}}{k}, \quad (20)$$

where  $f^{(N)} \equiv \frac{d \ln \delta_b^{(N)}}{d \ln a}$  is the linear growth factor and ‘ $N$ ’ means that the quantity is evaluated in Newtonian gauge. For conciseness, we will omit ‘ $N$ ’ in  $v_b^{(N)}$  in the following.

To estimate the magnitude of  $v_b$ , we first solve Eqs. (12)-(19) and derive the peculiar velocity of baryon in Newtonian gauge. Then we compute the root mean square (rms) dispersion of  $v_b$  within a sphere of radius  $r$  by

$$\langle v_b^2 \rangle = \int d^3k W_r^2(k) P_v(k), \quad (21)$$

where  $W_r(k)$  is a top hat window function of radius  $r$  and  $P_v(k)$  is the power spectrum of  $v_b$ . The magnitude  $\langle v_b^2 \rangle^{1/2}$  represents the mean velocity of baryons within a sphere of radius  $r$  with respect to the mean matter distribution. For comparison, we also compute the same magnitude for the fiducial  $\Lambda$ CDM model.

We present the calculated  $\langle v_b^2 \rangle^{1/2}$  at  $z = 0.1$  in the right column of Fig.1. We see that the velocity in the TeVeS model is larger than that in  $\Lambda$ CDM at the scale of 10Mpc, which is consistent with the fast growth rate displayed in the left column. Depending on the parameters,  $v_b$  in TeVeS can be as large as twice the  $\Lambda$ CDM value. With the increase of radius  $r$ , the velocity dispersion in the TeVeS model decays faster than in the  $\Lambda$ CDM model. When  $r$  reaches 100 Mpc, the velocity of the TeVeS models with small values of  $l_B$  and  $\mu_0$  can become lower than that of  $\Lambda$ CDM. In general smaller TeVeS parameters lead to lower velocity. This may be counterintuitive since  $\delta_b^{(N)} \simeq \delta_b$  grows faster for smaller TeVeS parameters. This is because  $v_b$  is proportional to the density perturbation  $\delta_b^{(N)}$  as well as the growth factor. With the decrease of TeVeS parameters,  $\delta_b^{(N)}$  is getting smaller. At  $z = 0.1$ ,

the influence of low density fluctuation overwhelms the high growth rate of baryons and the net effect is the decrease of  $v_b$ .

Observationally it is difficult to measure the peculiar velocity on scales above  $50h^{-1}\text{Mpc}$  using galaxies. The kSZ effect provides an alternative method of great promise to measure peculiar velocity at cosmological distances, without resorting to distance indicators. High resolution and low noise CMB experiments have the potential to measure various statistical averages of cluster velocity such as the bulk flow (e.g. [71, 72]), the mean pairwise momentum (e.g. [73]) and the momentum power spectrum (e.g. [74]). Advanced CMB experiments even have the capability of measuring the peculiar velocity of individual galaxy clusters (e.g. [75–80]). In [73] Hand *et al.* reported the measurement of the mean pairwise momentum of clusters using the CMB sky map made by the Atacama Cosmology Telescope (ACT). *Planck* found the radial peculiar velocity rms to be below three times the  $\Lambda\text{CDM}$  prediction at  $z = 0.15$  [81]. While the results from ACT and *Planck* seem to be consistent with the  $\Lambda\text{CDM}$  model, given their large uncertainties they are also compatible with TeVeS cosmology. To conclude, while at present the data do not have the statistical power to constrain the TeVeS parameters, the peculiar velocity field could become an important test of TeVeS theory with future data sets of higher resolution and lower noise.

### C. The kinetic Sunyaev-Zel'dovich effect

The Sunyaev-Zel'dovich (SZ) effect [82] is generated through the scattering of CMB photons by free electrons while the photons travel through ionized gas after reionization. The SZ effect is commonly classified into two sorts: the thermal SZ (tSZ) effect, which is characterized by the thermal motion of free electrons, and the kSZ effect, which is characterized by their bulk motion. Because free electrons produced after reionization of the intergalactic medium share the same motion as the plasma, it is expected that the kSZ effect can serve as a probe of baryon peculiar velocity field.

The kSZ effect induces distortions on the CMB temperature map. The kSZ temperature anisotropy is given by

$$\frac{\Delta T(\hat{\mathbf{n}})}{T_{\text{CMB}}} = - \int_{t_{\text{re}}}^{t_0} n_e \sigma_T e^{-\kappa} (\mathbf{v}_e^{(N)} \cdot \hat{\mathbf{n}}) dt, \quad (22)$$

where  $n_e$  is the electron density,  $\sigma_T$  is the Thomson cross section and  $\kappa$  is the Thomson optical depth, and  $\mathbf{v}_e^{(N)}$  is the peculiar velocity of free electrons; the integral is along the line of sight (l.o.s.) out to the reionization epoch and  $\hat{\mathbf{n}}$  is the unit vector along the l.o.s. The contribution of the kSZ effect to the CMB temperature angular power spectrum is [83–85]

$$C_l^{kSZ} = \frac{16\pi^2}{(2l+1)^3} (\bar{n}_e(0)\sigma_T)^2 \int_0^{z_{\text{re}}} (1+z)^4 \chi_e^2 \frac{1}{2} \Delta_B^2(k, z) |_{k=l/x} e^{-2\kappa} x(z) \frac{dx(z)}{dz} dz, \quad (23)$$

where  $x$  is the comoving distance,  $\bar{n}_e(0)$  is the mean electron number density at present,  $\chi_e$  is the ionization fraction and  $\Delta_B^2(k, z) \equiv \frac{k^3}{2\pi^2} P_B(k, z)$ .  $P_B$  is the power spectrum of the curl part of  $p \equiv (1 + \delta_e^{(N)}) \mathbf{v}_e^{(N)}$ . In the linear regime,  $\mathbf{v}_e^{(N)}$  is curl free and only the combination  $\delta_e^{(N)} \mathbf{v}_e^{(N)}$  contributes to  $P_B$ . Given  $\delta_e^{(N)} = \delta_b^{(N)}$ ,  $\mathbf{v}_e^{(N)} = \mathbf{v}_b$  and (20),  $P_B$  can be written as

$$P_B(k, z) = \frac{1}{2} \int \frac{d^3 \mathbf{k}'}{(2\pi)^3} \left( \frac{\dot{D}(z)}{D(z)} \right)^2 P(k', z) P(k - k', z) \times [W_g(k - k') \beta(\mathbf{k}, \mathbf{k}') + W_g(k') \beta(\mathbf{k}, \mathbf{k} - \mathbf{k}')]^2, \quad (24)$$

where  $D(z) \equiv \delta_b^{(N)}(z)/\delta_b^{(N)}(0)$  is the growth function of the baryon,  $P(k)$  is the baryon power spectrum in Newtonian gauge,  $W_g(k)$  is the transfer function that takes into account the suppression of baryon density fluctuations at small scales due to physical processes[86], and  $\beta(\mathbf{k}, \mathbf{k}') = [\mathbf{k}' - \mathbf{k}(\mathbf{k} \cdot \mathbf{k}')/k^2]/k'^2$ . For simplicity, we have set  $W_g(k)$  to unity in our numerical calculations.

The nonlinear evolution of density perturbations enhances the power spectrum at small scales. To account for this effect, we rewrite (24) into [84, 87, 88]

$$P_B(k, z) = \frac{1}{2} \int \frac{d^3 \mathbf{k}'}{(2\pi)^3} \left( \frac{\dot{D}}{D} \right)^2 P(k', z) P(k - k', z) \times [W_g(k - k') T_{NL}(k - k') \beta(\mathbf{k}, \mathbf{k}') + W_g(k') T_{NL}(k') \beta(\mathbf{k}, \mathbf{k} - \mathbf{k}')]^2, \quad (25)$$

where we have defined the nonlinear power spectrum as  $P^{NL}(k) \equiv P(k) T_{NL}^2(k)$ . It is assumed that the nonlinear corrections affect the density perturbation only and the velocity field is still linear[89]. [85] found that the other linear power spectrum should also be replaced by the nonlinear one to better describe the simulated  $\Delta_B^2$ . This is likely caused by the extra contribution from the curl velocity component generated by shell crossing. To include the nonlinear correction we need to specify  $T_{NL}(k)$  for the TeVeS model, which is usually done by using adequate fits to N-body simulations. However, such a simulation has not been carried out in TeVeS theory. It is then difficult to give a reliable description of the nonlinear corrections. As a first guess, we borrow the halofit fitting formula[90, 91] for  $\Lambda$ CDM model to evaluate the nonlinear power spectrum. We have to emphasize that this is only a rough estimation because TeVeS theory is significantly different from GR at cluster scales where the kSZ effect becomes important in the CMB anisotropies.

In Fig.2, we present the theoretical predictions of both linear and nonlinear kSZ power spectrum in the TeVeS model and the fiducial  $\Lambda$ CDM model. For consistency, we have assumed  $\tau = 0.09$  for all models. The solid lines represent the linear kSZ effect. The power spectra for TeVeS are always smaller than that of the  $\Lambda$ CDM model. Increasing the TeVeS parameters will further suppress the kSZ effect. Taking into account the nonlinear effect, the power spectra for TeVeS are enhanced and become comparable with the  $\Lambda$ CDM model. In contrast to the linear kSZ effect, increasing the TeVeS parameters enhances the power spectrum. The difference may be the consequence of the scale-dependent evolution of perturbations in TeVeS.  $T_{NL}(k)$  varies with  $k$ , which means that the main contributions to the linear and nonlinear kSZ power spectrum come from different scales. And the linear matter power spectrum  $P(k)$  at different scales changes differently when the parameters vary. Therefore the linear and nonlinear power spectra respond differently to the changing of the parameters. Again we emphasize that this phenomenon depends heavily on the estimation of  $P^{NL}(k)$ , and it is premature to make solid conclusion before we can have an accurate nonlinear matter power spectrum in TeVeS theory.

We include two data points for the kSZ power spectrum in Fig.2. The rectangle indicates the upper limit of  $D_l \equiv l(l+1)C_l/2\pi$  at  $l = 3000$  with 95% C.L. derived from ACT data,  $D_{3000}^{\text{kSZ}} < 8.6 \mu\text{K}^2$ [92]. The circle with the error bar indicates the measurement of the SPT-SZ survey using data from the South Pole Telescope(SPT),  $D_{3000}^{\text{kSZ}} = 2.9 \pm 1.3 \mu\text{K}^2$  with 68% C.L.[93]. These measurements heavily rely on modeling of cosmic infrared background and tSZ contributions, and therefore suffer from significant systematic uncertainty. Meanwhile our theoretical predictions have considerable uncertainties. Besides the nonlinear effect, we have assumed a simple instantaneous reionization model with  $\tau = 0.09$  while the kSZ effect

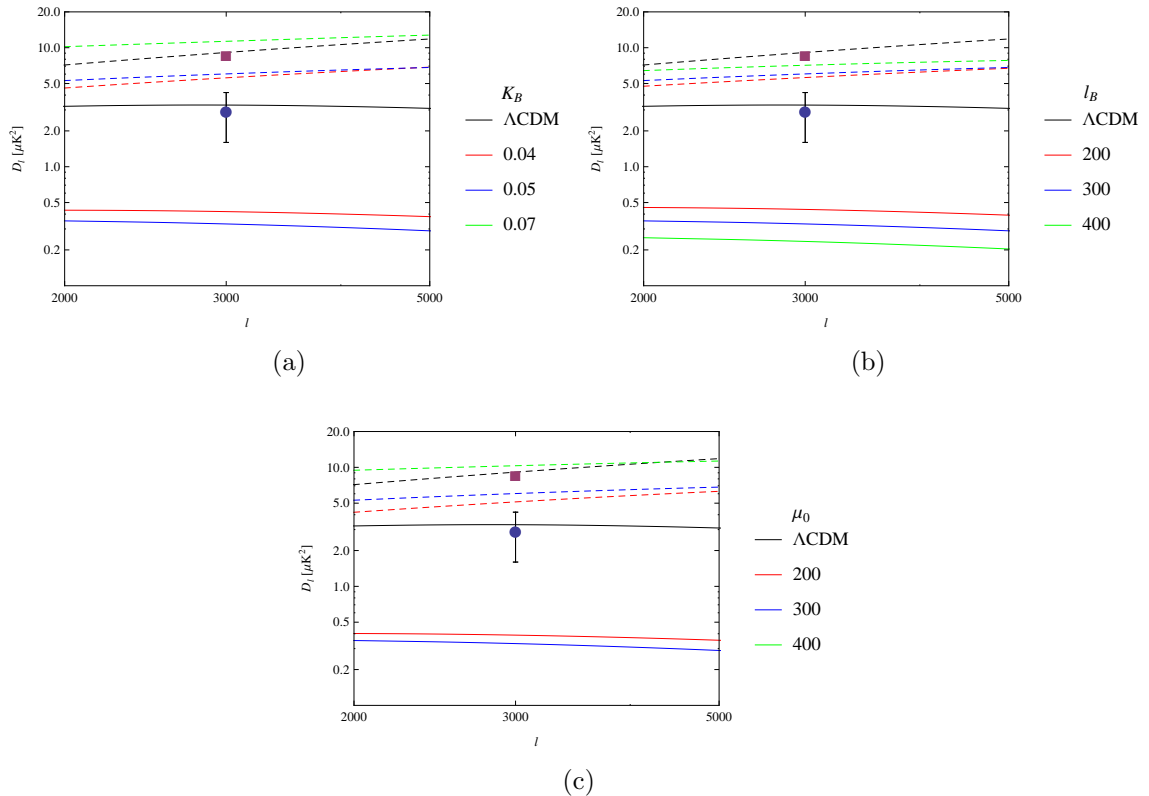


FIG. 2: The kSZ anisotropy power spectra for the TeVeS model with different parameters. The black curve is for the fiducial  $\Lambda\text{CDM}$  model. The solid lines represent the linear kSZ power spectra and the dashed lines are for the kSZ power spectra taking into account the nonlinear corrections. The TeVeS parameters are the same as in Fig.1 if not specified.

from the patchy reionization is expected to be important. Hence the kSZ power spectrum may be underestimated. Besides, that  $\tau$  in all models have the same value is a rough assumption itself, since a change in the rate of structure growth will also change the optical depth. On the other hand, we did not include the smoothing in the gas density caused by the gas pressure in our calculation, which could potentially reduce the amplitude of the kSZ power spectrum. And it is known that some fraction of the electrons is locked up in stars and neutral clouds, which further reduces the kSZ amplitude. Despite these uncertainties, our computations indicate that the linear kSZ power spectrum in the TeVeS model is consistent with the upper limits of the observations. The fact that it is smaller than the lower limit of SPT measurement does not rule out the TeVeS since the linear kSZ power spectrum is essentially a lower limit to the realistic one. But if we look at the nonlinear kSZ power spectra, they are certainly ruled out by the SPT observation, and the ACT measurement puts a tight constraint on the model parameters.

#### D. The scale dependence of growth rate

One of the characteristic features of the  $\Lambda\text{CDM}$  model is the scale-independent growth rate in the subhorizon approximation[94]. This property was found to be violated if the

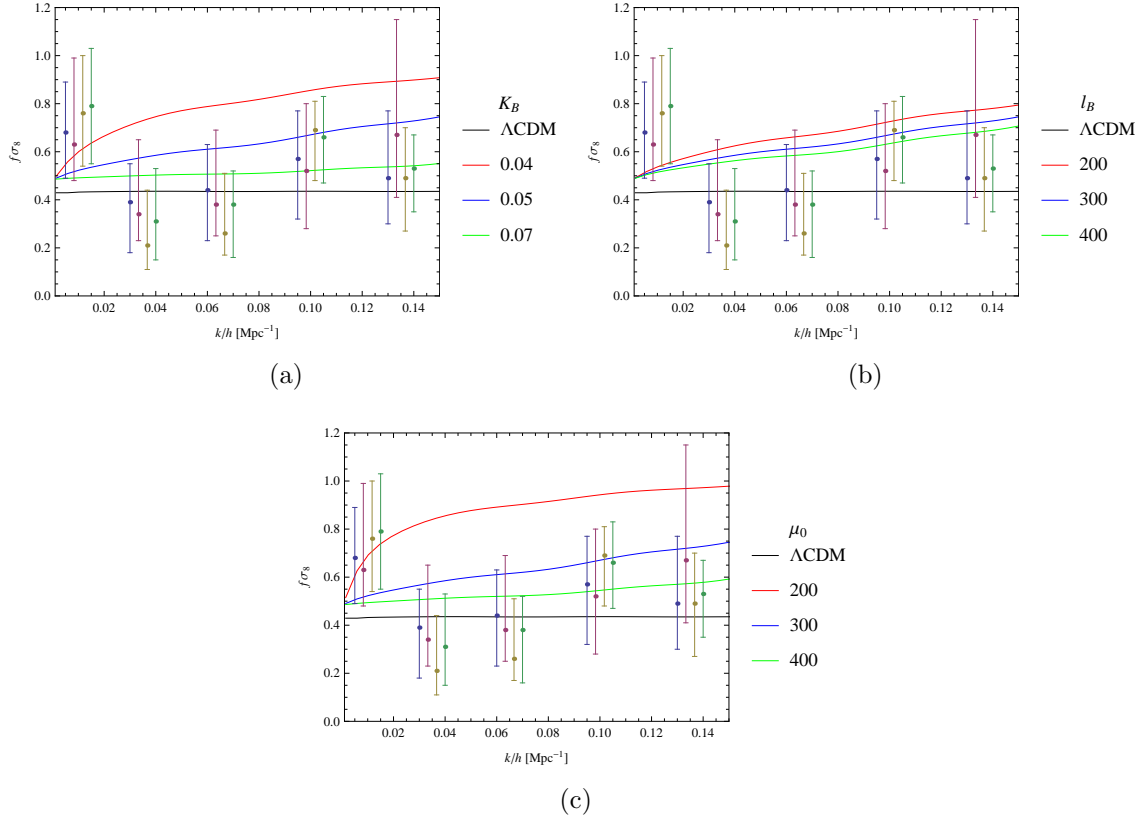


FIG. 3:  $f\sigma_8(k; z = 0)$  for the TeVeS model with different parameters. The black curve is for the fiducial  $\Lambda$ CDM model. The data points are from the 6-degree Field (6dF) Galaxy Survey. For all curves,  $\sigma_8(0) = 0.834$ .

gravity goes beyond GR[95–99], if DE clustering cannot be neglected[100, 101] or if DE couples to DM[102, 103]. Now we investigate the scale dependence of the growth rate in TeVeS theory and see whether it can serve to distinguish the TeVeS from the  $\Lambda$ CDM model.

Since observations are in fact sensitive to the normalized growth rate  $f\sigma_8(k; z)$  instead of  $f(k; z)$ , in Fig.3 we display  $f\sigma_8(k)$  in synchronous gauge for baryon with respect to  $k/h$  at redshift  $z = 0$ . In all models, we use the same value for  $\sigma_8(0)$ ,  $\sigma_8(0) = 0.834$ ; thus, we can concentrate on the scale dependence of the growth rate. It is a realistic assumption, since  $\sigma_8(0)$  in a viable cosmology model should be similar to that in the fiducial  $\Lambda$ CDM model. The growth rate in TeVeS is systematically higher than that in the  $\Lambda$ CDM model. The black curve for the fiducial  $\Lambda$ CDM model is almost a horizontal line, reflecting the scale-independent growth of density perturbations. In contrast to the  $\Lambda$ CDM model,  $f\sigma_8(k)$  in TeVeS theory clearly varies with scale. We see that the growth rate is bigger at small scales than large scales. Increasing the TeVeS parameters,  $f\sigma_8(k)$  at given  $k$  becomes smaller, which is consistent with the behavior seen in Fig.1. Furthermore,  $f\sigma_8(k)$  converges for different parameters when  $k \rightarrow 0$ , if  $\sigma_8$  is equally normalized.

We compare the theoretical prediction of  $f\sigma_8(k; z = 0)$  with the measurement using the observations of peculiar motions of galaxies of the 6-degree Field(6dF) Galaxy Survey velocity sample together with a newly compiled sample of low-redshift type Ia supernovae[59]. The measurement was done in 5  $k$  bins:  $k_1 = [0.005, 0.02]$ ,  $k_2 = [0.02, 0.05]$ ,  $k_3 = [0.05, 0.08]$ ,

$k_4 = [0.08, 0.12]$  and  $k_5 = [0.12, 0.15]$ . The data points in different color refer to results derived by different data sets and methodologies. The measurement does not show strong evidence for a scale dependence in the growth rate. But we see that the TeVeS prediction matches the measured  $f\sigma_8$  for a wide range of parameters.

Currently, the measurements of the scale dependence of growth rate is not as accurate as the average growth rate at different redshifts measured through redshift-space distortion observations. The latter has been used in the literature to constrain cosmological models(e.g. [104–106]). In this paper, we concentrated on the scale dependence of growth rate and hope that future precise data can help to constrain the TeVeS cosmological model.

#### IV. COSMIC MICROWAVE BACKGROUND RADIATION IN TEVES THEORY

In the last section, we investigated the structure growth in TeVeS cosmology. On the baryon peculiar velocity, kSZ effect, and scale dependence of growth rate, the theoretical predictions all exhibit clear difference between the TeVeS model and  $\Lambda$ CDM model. However in observations, current data are not precise and powerful enough to distinguish clearly the TeVeS model from the  $\Lambda$ CDM. In this section, we turn to study the CMB power spectrum in TeVeS cosmology. CMB experiments probe larger scales and deeper redshift of the Universe than large scale structure observations. Meanwhile, precise measurements of the CMB have been available. They can be used to tightly constrain the TeVeS model.

In [46], the first numerical calculation of CMB angular power spectrum in TeVeS theory was done by using the original Bekenstein’s potential (4). The authors found that a flat universe composed of about 5% baryon and 95% cosmological constant today matches the observations poorly. The angular distance relation was found modified as compared to the standard adiabatic  $\Lambda$ CDM universe. The positions of the peaks in the CMB angular power spectrum were observed shifted to higher  $l$ s which led to a severe mismatch with the observational data. This problem was argued to be cured if the three neutrinos have a mass of  $m_\nu \simeq 2\text{eV}$ [46]. In [60] it was argued that if including a sterile neutrino with  $\Omega_\nu \simeq 0.23$  ( $m_\nu \simeq 11\text{eV}$ ) in addition to the three massless neutrinos, the peaks of the CMB power spectrum will be located at the right positions to match the observational data. Furthermore by fitting a MOND-like model to the WMAP five year data, it was concluded that the model with the sterile neutrino is compatible with the observation. But in [60], it was assumed that there were no MOND effects before recombination; therefore, the MOND effects have no influence on the CMB power spectrum. It was commented that the fitting result in [60] has nothing to do with TeVeS features[26].

Here, we do the whole calculation in the framework of TeVeS theory. We numerically calculate the CMB power spectrum in TeVeS theory in the presence of a sterile neutrino. Our results are demonstrated in Fig.4. The black line is for the fiducial  $\Lambda$ CDM model. The red lines are for TeVeS models with various  $\Omega_\nu h^2$ . To illustrate the qualitative influence of the abundance of the sterile neutrino, we fix the parameters in the TeVeS models by taking  $K_B = 0.1$ ,  $l_B = 100$  and  $\mu_0 = 300$ . The other parameters are the same as in the fiducial  $\Lambda$ CDM model except that we have no CDM in TeVeS and  $\ln(10^{10} A_s)$  is adjusted such that the first peaks of the power spectra have the same height. The data points and error bars are from the *Planck* 2013 results[107]. It is clear in Fig.4 that including the fourth neutrino can move the locations of the acoustic peaks to larger angular scales. Moreover, it can also enhance the third acoustic peak to almost as high as the second peak, which is usually considered the signature of CDM in the Universe. With the increase of the abundance of

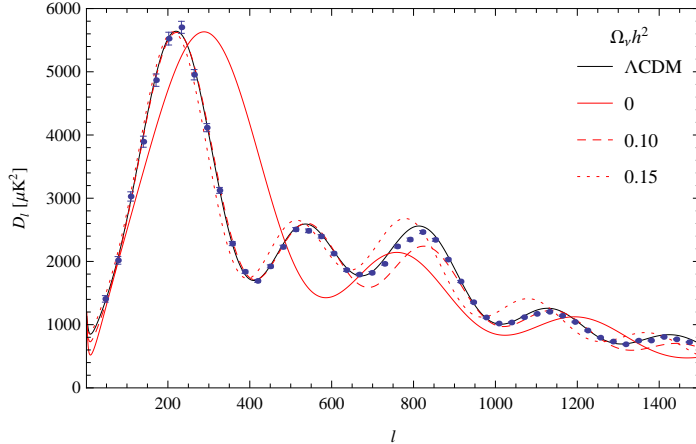


FIG. 4: The CMB temperature angular power spectra for the fiducial  $\Lambda$ CDM model (solid black curve) and TeVeS models (red curves) having various amounts of sterile neutrino. The data points with error bars are from *Planck* 2013 results.

TABLE I: The priors and fitting results of the cosmological parameters.

Parameter	Best fit	68% limits	Prior
$K_B$	0.0535	$< 0.0701$	[0.05, 0.5]
$l_B$	278	$> 229$	[10, 300]
$\mu_0$	326	$329^{+37}_{-41}$	[10, 400]
$\Omega_\nu h^2$	0.157	$0.156^{+0.003}_{-0.002}$	[0.01, 0.5]
$\Omega_b h^2$	0.0209	$0.0209 \pm 0.0002$	[0.01, 0.03]
$h$	0.504	$< 0.508$	[0.5, 0.85]
$\tau$	0.00390	$< 0.031$	[0, 0.3]
$n_s$	0.898	$0.900^{+0.005}_{-0.007}$	[0.8, 1.4]
$\ln(10^{10} A_s)$	2.89	$2.93^{+0.02}_{-0.06}$	[2.3, 3.5]

the fourth neutrino, there is clearly a competition between the shift of the peak positions and the enhancement of the third peak.

In [46], the authors found that changing the TeVeS parameters will modify the CMB power spectrum. It was observed that sufficiently small TeVeS parameters,  $K_B$ ,  $l_B$  and  $\mu_0$ , can cause the excess of the CMB power at large scales. Their conclusion was obtained in the absence of the sterile neutrino. We can see a similar property in Fig.5 where the fourth neutrino has an abundance of  $\Omega_\nu h^2 = 0.15$ . Smaller TeVeS parameters consistently enhance the large scale power in CMB. The CMB power spectrum at small  $l$ s is more sensitive to the parameter  $K_B$  than the other two parameters. Considering that  $K_B$  regulates the dynamics of the vector field, our observation here supports the argument in [47] that the vector field perturbation plays an important role in the growth of structure in the TeVeS. Furthermore, we display in Fig.5 that the influence of TeVeS parameters on the CMB power spectrum at small scales is totally overshadowed by that of the abundance of the fourth neutrino. The change of the positions and amplitudes of acoustic peaks is mainly caused by the change of  $\Omega_\nu h^2$ .

In order to test the viability of TeVeS theory in explaining the observed CMB power spec-

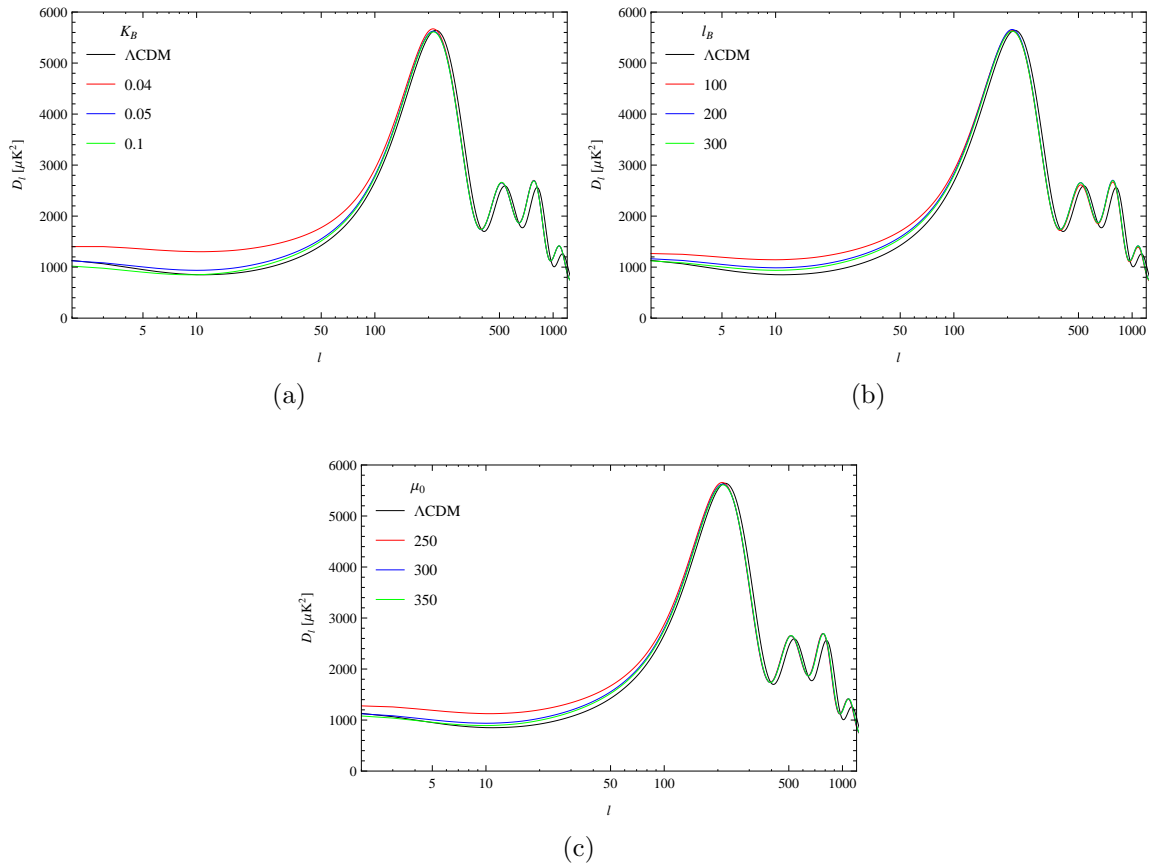


FIG. 5: The CMB temperature angular power spectra for TeVeS models with different parameters. The black curve is for the fiducial  $\Lambda$ CDM model. The TeVeS parameters are  $K_B = 0.05$ ,  $l_B = 300$  and  $\mu_0 = 300$  if not specified. The fourth neutrino abundance is  $\Omega_\nu h^2 = 0.15$

trum and constrain the TeVeS parameters as well as the amount of the sterile neutrino, we confront the TeVeS model with the *Planck* 2013 results[107]. The data set we used includes the CMB TT power spectrum for  $2 \leq l \leq 2500$ . We perform the numerical fitting using the Markov chain Monte Carlo method. In the fitting, we allow nine parameters to vary, which are  $K_B$ ,  $l_B$ ,  $\mu_0$ ,  $\Omega_\nu h^2$ ,  $\Omega_b h^2$ ,  $h$ ,  $\tau$ ,  $n_s$ , and  $\ln(10^{10} A_s)$ . The priors of these parameters are listed in the last column in Table I. We modify the public code CMBEASY[108] to compute the CMB power spectra and generate the Markov chains.

The TeVeS parameters have a similar influence on the CMB. The CMB power spectrum for large  $l$ s hardly depends on  $K_B$ ,  $l_B$  or  $\mu_0$ , while the low- $l$  power is suppressed when one of the TeVeS parameters increases. So one expects degeneracy among them when fitting to the CMB observations. Nevertheless, we can get moderate constraints for them by using *Planck* data alone, as indicated in Table I.

Comparing with the  $\Lambda$ CDM model, the constrained optical depth to the last scattering surface in the TeVeS model is significantly smaller. Inferring from *Planck* data, the 68% C.L. for the optical depth is  $\tau = 0.09 \pm 0.038$  for the  $\Lambda$ CDM model[109]. Assuming instantaneous reionization, the best-fit value for the TeVeS model,  $\tau = 0.0039$ , implies that reionization completed at  $z = 1.2$ . This is certainly ruled out by astronomical observations which suggests



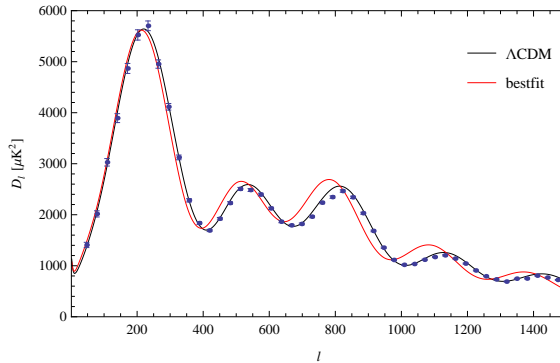


FIG. 6: The CMB temperature angular power spectra for the best-fit TeVeS model (red) and the fiducial  $\Lambda$ CDM model (black). The data points with error bars are from *Planck* 2013 results.

the end of reionization was at  $z \simeq 6$  or earlier. But if we take the 68% C.L.  $\tau = 0.31$ , the situation becomes better. The end of reionization was at  $z = 6.2$ . Thus, TeVeS cosmology is still marginally allowed by current constraints of reionization history.

It is interesting that the constrained abundance of the sterile neutrino,  $\Omega_\nu h^2 = 0.156_{-0.002}^{+0.003}$ , which corresponds to  $m_\nu \simeq 15\text{eV}$ , is larger than the CDM abundance ( $\simeq 0.12$ ) gotten in concordance with the  $\Lambda$ CDM model[109]. Meanwhile, the obtained  $h$  is much smaller than the prediction in [60]. Recall that the locations of the acoustic peaks shift towards smaller  $l$  when  $\Omega_\nu h^2$  increases; see Fig.4. This explains why our constraint on  $H_0$  is so small. When Hubble's constant decreases, the angular diameter distance to the last scattering surface is increased. Thus, the angular scales of the acoustic peaks are reduced, which compensates the effect of excessive  $\Omega_\nu h^2$ . Actually, the best-fit value of  $h = 0.504$  resides at the edge of the prior. One may expect that it will become even smaller if the lower limit of the prior is decreased, and therefore the best-fit  $\Omega_\nu h^2$  becomes larger. Obviously this is in severe conflict with measurements using supernova observations,  $H_0 = 73.8 \pm 2.4 \text{km} \cdot \text{s}^{-1} \cdot \text{Mpc}^{-1}$ [110].

To test the goodness of the fit, we computed the  $\chi^2$  of the best-fit TeVeS model and found  $\chi^2 = 8292.54$ . For comparison, the  $\Lambda$ CDM best fit gives  $\chi^2 = 7791.18$ [111]. The difference is  $\Delta\chi^2 = 501.36$ . This is strong evidence that the TeVeS model considered in this paper cannot explain current CMB measurements. The difference in the  $\chi^2$ s is especially impressing, considering that the degree of freedom in the TeVeS is significantly increased. The original TeVeS model with a sterile neutrino is then ruled out by CMB observations. In Fig.6 we can see that the best fit TeVeS model cannot properly fit the high- $l$  CMB power spectrum from *Planck*. Considering that  $\Omega_\nu h^2$  has an important influence on the high- $l$  CMB power spectrum and its large best-fit value, this may suggest that the sterile neutrino is not a satisfactory substitute of DM in TeVeS cosmology.

## V. CONCLUSIONS

In this paper we have tested the TeVeS theory with several cosmological observations. We have extended the previous probe of the late time structure growth by measuring the ratio of different perturbations  $E_G$  in [48] to the complementary observations by measuring the overall amplitude of perturbations, such as the velocity spectrum and the kSZ effect, respectively. We have found that the dispersion of the baryon peculiar velocity at  $r <$

100Mpc in the TeVeS cosmology is usually larger than that in the  $\Lambda$ CDM model and  $\langle v_b^2 \rangle$  decays faster in the TeVeS when the scale increases. We have computed the linear and nonlinear kSZ anisotropy power spectrum in TeVeS theory by assuming  $\tau = 0.09$ . The linear kSZ power spectra are within upper limits measured by SPT and ACT, although they are much lower than those of the  $\Lambda$ CDM model. The nonlinear kSZ power spectrum in the TeVeS model is in tension with measurements of the SPT and ACT, despite the uncertainties in our theoretical prediction.

We have extended our discussions to the scale dependence of the evolution of large scale structure. In TeVeS cosmology, we have shown that the normalized growth rate  $f\sigma_8(k)$  rises with the increase of  $k$  at  $z = 0$ . This is clearly in contrast to the scale-independent growth at subhorizon scales in the  $\Lambda$ CDM model. Although the predicted  $f\sigma_8$  in TeVeS theory is consistent with the current measurement using 6dF data, we expect that the distinct scale dependence of the growth rate in the TeVeS model can potentially serve as a powerful probe in distinguishing the TeVeS from GR in future observations.

Considering the available high precision data on the cosmic microwave background radiations, we have studied the CMB power spectrum in a TeVeS universe containing a sterile neutrino. Fitting to *Planck* 2013 data, we noticed that for the TeVeS cosmology, although the constrained optical depth at the border of the 68% C.L. can give the end of the reionization marginally allowed by the constraints on the reionization history of our Universe, the best fit value of the optical depth is extremely small, which indicates that the end of reionization happened at  $z = 1.2$ . The constraints for the abundance of the sterile neutrino and the Hubble's constant read  $\Omega_\nu h^2 = 0.156^{+0.003}_{-0.002}$  and  $H_0 < 50.8 \text{ km} \cdot \text{s}^{-1} \cdot \text{Mpc}^{-1}$  at 68% C.L. The obtained Hubble parameter is much lower than the observed value from supernovae measurements. This is certainly not allowed and it clearly rules out the TeVeS model considered in this work. Furthermore, comparing the  $\chi^2$  of the best-fit TeVeS model with that of  $\Lambda$ CDM, we find that the TeVeS model is significantly disfavored by CMB observations. Because of the large uncertainties in current observations, the statistical significance of measurements of the kSZ effect and growth rate is now much weaker than CMB observations such as *Planck*. Yet we expect, with the improvement of the accuracy in their measurements, they will be useful in constraining cosmological models and become good complementary probes to CMB measurements.

In conclusion, we have examined the late time structure growth in the TeVeS model and found tensions between the TeVeS and cosmological observations. The conflict is more obvious when the TeVeS model is confronted by the CMB observations from *Planck*. Although the current available observational data from large scale structure growth are not precise enough to put tight constraints on the TeVeS model, our theoretical discussions on the density growth rate and its scale dependence in the TeVeS model can demonstrate that these complementary observable quantities have prospective abilities to distinguish general relativity and modified gravity theories at cosmological scales. With upcoming precise measurements, more studies in this respect are called for.

## ACKNOWLEDGMENTS

We acknowledge financial support from National Basic Research Program of China (973 Program 2013CB834900 & 2015CB857001) and National Natural Science Foundation of

- 
- [1] J. Oort, *Bull. Astron. Inst. Neth.* **6**, 249 (1932).
  - [2] F. Zwicky, *Helvetica Physica Acta* **6**, 110 (1933).
  - [3] S. Smith, *Astrophys. J.* **83**, 23 (1936).
  - [4] V. C. Rubin and J. W. K. Ford, *Astrophys. J.* **159**, 379 (1970).
  - [5] V. C. Rubin, N. Thonnard, and J. W. K. Ford, *Astrophys. J.* **238**, 471 (1980).
  - [6] B. P. Schmidt, N. B. Suntzeff, M. M. Phillips, R. A. Schommer, A. Clocchiatti, R. P. Kirshner, P. Garnavich, P. Challis, B. Leibundgut, J. Spyromilio, A. G. Riess, A. V. Filippenko, M. Hamuy, R. C. Smith, C. Hogan, C. Stubbs, A. Diercks, D. Reiss, R. Gilliland, J. Tonry, J. Maza, A. Dressler, J. Walsh, and R. Ciardullo, *Astrophys. J.* **507**, 46 (1998).
  - [7] S. Perlmutter, G. Aldering, G. Goldhaber, R. Knop, P. Nugent, P. Castro, S. Deustua, S. Fabbro, A. Goobar, D. Groom, I. M. Hook, A. Kim, M. Kim, J. Lee, N. Nunes, R. Pain, C. Pennypacker, R. Quimby, C. Lidman, R. Ellis, M. Irwin, R. McMahon, P. Ruiz-Lapuente, N. Walton, B. Schaefer, B. Boyle, A. Filippenko, T. Matheson, A. Fruchter, N. Panagia, H. Newberg, and W. Couch, *Astrophys. J.* **517**, 565 (1999).
  - [8] Y. Sofue and V. Rubin, *Ann. Rev. Astron. Astrophys.* **39**, 137 (2001).
  - [9] D. Clowe, M. Bradac, A. H. Gonzalez, M. Markevitch, S. W. Randall, C. Jones, and D. Zaritsky, *Astrophys. J.* **648**, L109 (2006).
  - [10] M. R.olta, J. Dunkley, R. S. Hill, G. Hinshaw, E. Komatsu, D. Larson, L. Page, D. N. Spergel, C. L. Bennett, B. Gold, N. Jarosik, N. Odegard, J. L. Weiland, E. Wollack, M. Halpern, A. Kogut, M. Limon, S. S. Meyer, G. S. Tucker, and E. L. Wright, *Astrophys. J. Suppl.* **180**, 296 (2009).
  - [11] M. Milgrom, *Astrophys. J.* **270**, 365 (1983).
  - [12] M. Milgrom, *Astrophys. J.* **270**, 371 (1983).
  - [13] M. Milgrom, *Astrophys. J.* **270**, 384 (1983).
  - [14] M. Milgrom and E. Braun, *Astrophys. J.* **334**, 130 (1988).
  - [15] K. G. Begeman, A. H. Broeils, and R. H. Sanders, *Mon. Not. R. Astron. Soc.* **249**, 523 (1991).
  - [16] R. H. Sanders, *Astrophysical Journal* **473**, 117 (1996).
  - [17] W. J. G. de Blok and S. S. McGaugh, *Astrophys. J.* **508**, 132 (1998).
  - [18] S. S. McGaugh and W. J. G. de Blok, *Astrophys. J.* **499**, 66 (1998).
  - [19] M. Milgrom and R. H. Sanders, *Mon. Not. R. Astron. Soc.* **357**, 45 (2005).
  - [20] M. Milgrom and R. H. Sanders, *Astrophys. J.* **658**, L17 (2007).
  - [21] S. S. McGaugh, J. M. Schombert, G. D. Bothun, and W. J. G. de Blok, *Astrophys. J.* **533**, L99 (2000).
  - [22] S. S. McGaugh, *Astrophys. J.* **632**, 859 (2005).
  - [23] R. H. Sanders, *Astron. Astrophys. Rev.* **2**, 1 (1990).
  - [24] M. Milgrom, in *Dark matter in astrophysics and particle physics, 1998*, edited by H. V. Klapdor-Kleingrothaus and L. Baudis (Institute of Physics Pub. (Philadelphia, PA), 1999) p. 443.
  - [25] R. H. Sanders and S. S. McGaugh, *Ann. Rev. Astron. Astrophys.* **40**, 263 (2002).
  - [26] C. Skordis, *Class.Quant.Grav.* **26**, 143001 (2009).
  - [27] V. Cardone, G. Angus, A. Diaferio, C. Tortora, and R. Molinaro, *MNRAS* **412**, 2617 (2011).

- [28] B. Famaey and S. McGaugh, *Living Reviews in Relativity* **15**, 10 (2012).
- [29] J. Bekenstein and M. Milgrom, *ApJ* **286**, 7 (1984).
- [30] J. D. Bekenstein, *Physics Letters B* **202**, 497 (1988).
- [31] R. H. Sanders, *MNRAS* **235**, 105 (1988).
- [32] J. D. Bekenstein and R. H. Sanders, *ApJ* **429**, 480 (1994).
- [33] R. H. Sanders, *ApJ* **480**, 492 (1997).
- [34] J. D. Bekenstein, *Phys.Rev. D* **70**, 083509 (2004).
- [35] I. Ferreras, M. Sakellariadou, and M. F. Yusaf, *Physical Review Letters* **100**, 031302 (2008).
- [36] I. Ferreras, N. E. Mavromatos, M. Sakellariadou, and M. F. Yusaf, *Phys. Rev. D* **80**, 103506 (2009).
- [37] N. E. Mavromatos, M. Sakellariadou, and M. F. Yusaf, *Phys. Rev. D* **79**, 081301 (2009).
- [38] M.-C. Chiu, C.-M. Ko, and Y. Tian, *ApJ* **636**, 565 (2006).
- [39] D.-M. Chen and H. Zhao, *ApJ* **650**, L9 (2006).
- [40] H. Y. Shan, M. Feix, B. Famaey, and H. Zhao, *MNRAS* **387**, 1303 (2008).
- [41] D.-M. Chen, *JCAP* **1**, 6 (2008).
- [42] M. Feix, H. Zhao, C. Fedeli, J. L. Pestana, and H. Hoekstra, *Phys. Rev. D* **82**, 124003 (2010).
- [43] M.-C. Chiu, C.-M. Ko, Y. Tian, and H. Zhao, *Phys.Rev.D* **83**, 063523 (2011).
- [44] M. Chaichian, J. Kluson, M. Oksanen, and A. Tureanu, *Phys.Lett.B* **735**, 322 (2014).
- [45] C. Skordis, *Phys.Rev.D* **74**, 103513 (2006).
- [46] C. Skordis, D. F. Mota, P. G. Ferreira, and C. Boehm, *Phys. Rev. Lett.* **96**, 011301 (2006).
- [47] S. Dodelson and M. Liguori, *Phys.Rev.Lett.* **97**, 231301 (2006).
- [48] R. Reyes, R. Mandelbaum, U. Seljak, T. Baldauf, J. E. Gunn, L. Lombriser, and R. E. Smith, *Nature* **464**, 256 (2010).
- [49] P. Zhang, M. Liguori, R. Bean, and S. Dodelson, *Phys.Rev.Lett.* **99**, 141302 (2007).
- [50] P. Bull, T. Clifton, and P. G. Ferreira, *Phys. Rev. D* **85**, 024002 (2012).
- [51] R. Genova-Santos, F. Atrio-Barandela, J. Muecket, and J. Klar, *Astrophys.J.* **700**, 447 (2009).
- [52] P. Zhang, *MNRAS Letters*, **407**, L36 (2010).
- [53] X.-D. Xu, B. Wang, P. Zhang, and F. Atrio-Barandela, *Journal of Cosmology and Astroparticle Physics* **12**, 001 (2013).
- [54] F. Beutler, S. Saito, H.-J. Seo, J. Brinkmann, K. S. Dawson, D. J. Eisenstein, A. Font-Ribera, S. Ho, C. K. McBride, F. Montesano, W. J. Percival, A. J. Ross, N. P. Ross, L. Samushia, D. J. Schlegel, A. G. Snchez, J. L. Tinker, and B. A. Weaver, *Monthly Notices of the Royal Astronomical Society* **443**, 1065 (2014).
- [55] C. Blake, S. Brough, M. Colless, C. Contreras, W. Couch, S. Croom, T. Davis, M. J. Drinkwater, K. Forster, D. Gilbank, M. Gladders, K. Glazebrook, B. Jelliffe, R. J. Jurek, I. hui Li, B. Madore, C. Martin, K. Pimblet, G. Poole, M. Pracy, R. Sharp, E. Wisnioski, D. Woods, T. Wyder, and H. Yee, *MNRAS* **415**, 2876 (2011).
- [56] S. de la Torre, L. Guzzo, J. A. Peacock, E. Branchini, A. Iovino, B. R. Granett, U. Abbas, C. Adami, S. Arnouts, J. Bel, M. Bolzonella, D. Bottini, A. Cappi, J. Coupon, O. Cucciati, I. Davidzon, G. D. Lucia, A. Fritz, P. Franzetti, M. Fumana, B. Garilli, O. Ilbert, J. Krywult, V. L. Brun, O. L. Fevre, D. Maccagni, K. Malek, F. Marulli, H. J. McCracken, L. Moscardini, L. Paioro, W. J. Percival, M. Polletta, A. Pollo, H. Schlegelhauser, M. Scodreggio, L. A. M. Tasca, R. Tojeiro, D. Vergani, A. Zanichelli, A. Burden, C. D. Porto, A. Marchetti, C. Marinoni, Y. Mellier, P. Monaco, R. C. Nichol, S. Phleps, M. Wolk, and G. Zamorani, *A&A* **557**,

- A54 (2013).
- [57] R. Bean and M. Tangmatitham, *Phys.Rev.D* **81**, 083534 (2010).
  - [58] S. F. Daniel and E. V. Linder, *JCAP* **02**, 007 (2013).
  - [59] A. Johnson, C. Blake, J. Koda, Y.-Z. Ma, M. Colless, M. Crocce, T. M. Davis, H. Jones, J. R. Lucey, C. Magoulas, J. Mould, M. Scrimgeour, and C. M. Springob, *Monthly Notices of the Royal Astronomical Society* **444**, 3926 (2014).
  - [60] G. W. Angus, *MNRAS* **394**, 527 (2009).
  - [61] D. Giannios, *Phys.Rev. D* **71**, 103511 (2005).
  - [62] F. Bourliot, P. G. Ferreira, D. F. Mota, and C. Skordis, *Phys.Rev.D* **75**, 063508 (2007).
  - [63] E. Sagi and J. D. Bekenstein, *Phys. Rev. D* **77**, 024010 (2008).
  - [64] R. H. Sanders, *Monthly Notices of the Royal Astronomical Society* **370**, 1519 (2006).
  - [65] G. W. Angus, B. Famaey, and H. S. Zhao, *Monthly Notices of the Royal Astronomical Society* **371**, 138 (2006).
  - [66] L. M. Diaz-Rivera, L. Samushia, and B. Ratra, *Physical Review D*, vol. **73**, 083503 (2006).
  - [67] P. G. Ferreira, C. Skordis, and C. Zunckel, *Phys.Rev.D* **78**, 044043 (2008).
  - [68] H. Zhao, *Int.J.Mod.Phys.D* **16**, 2055 (2007).
  - [69] J. G. Hao and R. Akhoury, *Int. J. Mod. Phys. D* **18**, 1039 (2009).
  - [70] C. Skordis, *Phys.Rev.D* **77**, 123502 (2008).
  - [71] A. Kashlinsky and F. Atrio-Barandela, *ApJ* **536**, L67 (2000).
  - [72] F. Atrio-Barandela, A. Kashlinsky, and J. P. Mücke, *Astrophys.J.* **601**, L111 (2004).
  - [73] N. Hand, G. E. Addison, E. Aubourg, N. Battaglia, E. S. Battistelli, D. Bizyaev, J. R. Bond, H. Brewington, J. Brinkmann, B. R. Brown, S. Das, K. S. Dawson, M. J. Devlin, J. Dunkley, R. Dunner, D. J. Eisenstein, J. W. Fowler, M. B. Gralla, A. Hajian, M. Halpern, M. Hilton, A. D. Hincks, R. Hlozek, J. P. Hughes, L. Infante, K. D. Irwin, A. Kosowsky, Y.-T. Lin, E. Malanushenko, V. Malanushenko, T. A. Marriage, D. Marsden, F. Menanteau, K. Moodley, M. D. Niemack, M. R. Nolta, D. Oravetz, L. A. Page, N. Palanque-Delabrouille, K. Pan, E. D. Reese, D. J. Schlegel, D. P. Schneider, N. Sehgal, A. Shelden, J. Sievers, C. Sifon, A. Simmons, S. Snedden, D. N. Spergel, S. T. Staggs, D. S. Swetz, E. R. Switzer, H. Trac, B. A. Weaver, E. J. Wollack, C. Yeche, and C. Zunckel, *Phys. Rev. Lett.* **109**, 041101 (2012).
  - [74] P. Zhang, H. A. Feldman, R. Juskiewicz, and A. Stebbins, *MNRAS* **388**, 884 (2008).
  - [75] M. G. Haehnelt and M. Tegmark, *Mon.Not.Roy.Astron.Soc.* **279**, 545 (1996).
  - [76] N. Aghanim, K. M. Grski, and J. L. Puget, *Astronomy and Astrophysics* **374**, 1 (2001).
  - [77] G. P. Holder, *ApJ* **602**, 18 (2004).
  - [78] L. Knox, G. Holder, and S. Church, *Astrophys.J.* **612**, 96 (2004).
  - [79] N. Aghanim, S. H. Hansen, and G. Lagache, *Astronomy and Astrophysics* **439**, 901 (2005).
  - [80] A. Diaferio, S. Borgani, L. Moscardini, G. Murante, K. Dolag, V. Springel, G. Tormen, L. Tornatore, and P. Tozzi, *MNRAS* **356**, 1477 (2005).
  - [81] Planck Collaboration, *A&A* **561**, A97 (2014).
  - [82] R. A. Sunyaev and Y. B. Zeldovich, *Comments on Astrophysics and Space Physics* **4**, 173 (1972).
  - [83] E. T. Vishniac, *Astrophys.J.* **322**, 597 (1987).
  - [84] C.-P. Ma and J. N. Fry, *Phys.Rev.Lett.* **88**, 211301 (2002).
  - [85] P. Zhang, U.-L. Pen, and H. Trac, *Mon.Not.Roy.Astron.Soc.* **347**, 1224 (2004).
  - [86] L.-Z. Fang, H. Bi, S. Xiang, and G. Boerner, *ApJ* **413**, 477 (1993).
  - [87] W. Hu, *Astrophys.J.* **529**, 12 (2000).

- [88] L. D. Shaw, D. H. Rudd, and D. Nagai, *ApJ* **756**, 15 (2012).
- [89] P. Coles and B. Jones, *MNRAS* **248**, 1 (1991).
- [90] R. E. Smith, J. A. Peacock, A. Jenkins, S. D. M. White, C. S. Frenk, F. R. Pearce, P. A. Thomas, G. Efstathiou, H. M. P. Couchmann, and T. V. Consortium, *Mon. Not. Roy. Astron. Soc.* **341**, 1311 (2003).
- [91] R. Takahashi, M. Sato, T. Nishimichi, A. Taruya, and M. Oguri, *The Astrophysical Journal* **761**, 152 (2012).
- [92] J. L. Sievers, R. A. Hlozek, M. R. Nolta, V. Acquaviva, G. E. Addison, P. A. R. Ade, P. Aguirre, M. Amiri, J. W. Appel, L. F. Barrientos, E. S. Battistelli, N. Battaglia, J. R. Bond, B. Brown, B. Burger, E. Calabrese, J. Chervenak, D. Crichton, S. Das, M. J. Devlin, S. R. Dicker, W. B. Doriese, J. Dunkley, R. Dnner, T. Essinger-Hileman, D. Faber, R. P. Fisher, J. W. Fowler, P. Gallardo, M. S. Gordon, M. B. Gralla, A. Hajian, M. Halpern, M. Hasselfield, C. Hernandez-Monteagudo, J. C. Hill, G. C. Hilton, M. Hilton, A. D. Hincks, D. Holtz, K. M. Huffenberger, D. H. Hughes, J. P. Hughes, L. Infante, K. D. Irwin, D. R. Jacobson, B. Johnstone, J. B. Juin, M. Kaul, J. Klein, A. Kosowsky, J. M. Lau, M. Limon, Y.-T. Lin, T. Louis, R. H. Lupton, T. A. Marriage, D. Marsden, K. Martocci, P. Mausekopf, M. McLaren, F. Menanteau, K. Moodley, H. Moseley, C. B. Netterfield, M. D. Niemack, L. A. Page, W. A. Page, L. Parker, B. Partridge, R. Plimpton, H. Quintana, E. D. Reese, B. Reid, F. Rojas, N. Sehgal, B. D. Sherwin, B. L. Schmitt, D. N. Spergel, S. T. Staggs, O. Stryzak, D. S. Swetz, E. R. Switzer, R. Thornton, H. Trac, C. Tucker, M. Uehara, K. Visnjic, R. Warne, G. Wilson, E. Wollack, Y. Zhao, and C. Zuncke, *JCAP* **10**, 060 (2013).
- [93] E. M. George, C. L. Reichardt, K. A. Aird, B. A. Benson, L. E. Bleem, J. E. Carlstrom, C. L. Chang, H.-M. Cho, T. M. Crawford, A. T. Crites, T. de Haan, M. A. Dobbs, J. Dudley, N. W. Halverson, N. L. Harrington, G. P. Holder, W. L. Holzappel, Z. Hou, J. D. Hrubes, R. Keisler, L. Knox, A. T. Lee, E. M. Leitch, M. Lueker, D. Luong-Van, J. J. McMahon, J. Mehl, S. S. Meyer, M. Millea, L. M. Mocuano, J. J. Mohr, T. E. Montroy, S. Padin, T. Plagge, C. Pryke, J. E. Ruhl, K. K. Schaffer, L. Shaw, E. Shirokoff, H. G. Spieler, Z. Staniszewski, A. A. Stark, K. T. Story, A. van Engelen, K. Vanderlinde, J. D. Vieira, R. Williamson, and O. Zahn, *ApJ* **799**, 177 (2015).
- [94] P. Zhang, *Phys.Rev.D* **83**, 063510 (2011).
- [95] C. Brans and R. H. Dicke, *Physical Review* **124**, 925 (1961).
- [96] G. Dvali, G. Gabadadze, and M. Porrati, *Phys. Lett. B* **485**, 208 (2000).
- [97] A. Nicolis, R. Rattazzi, and E. Trincherini, *Phys.Rev.D* **79**, 064036 (2009).
- [98] S. Tsujikawa, *Lect. Notes Phys.* **800**, 99 (2011).
- [99] T. Clifton, P. G. Ferreira, A. Padilla, and C. Skordis, *Physics Reports* **513**, 1 (2012).
- [100] P. Creminelli, G. D'Amico, J. Norea, and F. Vernizzi, *JCAP* **02**, 018 (2009).
- [101] K. Parfrey, L. Hui, and R. K. Sheth, *Phys.Rev.D* **83**, 063511 (2011).
- [102] J.-H. He, B. Wang, and Y. P. Jing, *JCAP* **07**, 030 (2009).
- [103] J.-H. He, B. Wang, E. Abdalla, and D. Pavon, *JCAP* **12**, 022 (2010).
- [104] S. Tsujikawa, A. D. Felice, and J. Alcaniz, *JCAP* **01**, 030 (2013).
- [105] E. Macaulay, I. K. Wehus, and H. K. Eriksen, *Phys. Rev. Lett.* **111**, 161301 (2013).
- [106] V. Salvatelli, N. Said, M. Bruni, A. Melchiorri, and D. Wands, *Phys. Rev. Lett.* **113**, 181301 (2014).
- [107] Planck Collaboration, *A&A* **571**, A15 (2014).
- [108] M. Doran, *JCAP* **06**, 011 (2005).
- [109] Planck Collaboration, *A&A* **571**, A16 (2014).

- [110] A. G. Riess, L. Macri, S. Casertano, H. Lampeitl, H. C. Ferguson, A. V. Filippenko, S. W. Jha, W. Li, and R. Chornock, *ApJ* **730**, 119 (2011).
- [111] Planck Collaboration, “Planck 2013 results. web-based explanatory supplement,” (2013).